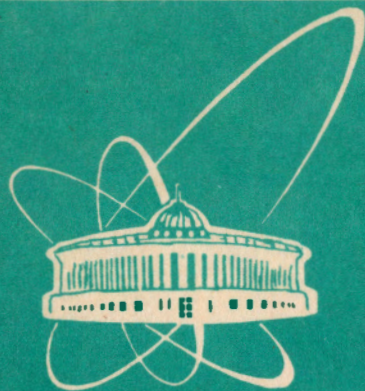


93-6



СООБЩЕНИЯ  
ОБЪЕДИНЕННОГО  
ИНСТИТУТА  
ЯДЕРНЫХ  
ИССЛЕДОВАНИЙ  
ДУБНА

E13-93-6

E.Dermendjiev, V.M.Nazarov, S.S.Pavlov,  
Iv.Ruskov, Yu.S.Zamyatnin

AN EXPERIMENTAL FACILITY  
FOR STUDYING DELAYED NEUTRON EMISSION

1993

## I. Introduction

The effective fraction of delayed neutrons,  $\beta_{eff} = \nu_{DN}/\nu$ , is one of the principal reactor physics constants, important for nuclear reactor designing, nuclear safeguards etc. Here  $\nu_{DN}$  is the total yield of delayed neutrons (DN) per fission,  $\nu$  is the average number of prompt fission neutrons per fission. Most of the measured  $\nu_{DN}$ -values for various fissioning isotopes were discussed and evaluated by Keepin [1], Tuttle [2], Sluhevskaja et al. [3] and by Blachot et al. [4]. Recently, Filip and D'Angelo [5] have shown that owing to the permanent progress in nuclear reactor technology measurements of enhanced accuracy are required of  $\nu_{DN}(th)$ -values for thermal neutron induced fission.

In order to meet such requirements a new experimental facility based on utilization of the Dubna IBR-2 pulsed reactor (PR), the slow neutron chopper (SNC) and a  $^3He$ -filled multicounter neutron detector (ND) was designed and tested for measuring  $\nu_{DN}(th)$ . Below a method for performing DN measurements and the experimental facility are briefly described. Certain results of test measurements performed with the SNC and the ND are discussed. Other applications of our facility are also briefly considered. The results of our  $\nu_{DN}(th)$  measurements for  $^{235}U$  will be reported elsewhere.

### II.A method of delayed neutron measurements

Most experimental methods for determining  $\nu_{DN}$  values involve a single irradiation of a target by neutrons and subsequent measurements of DN emission [2]. By setting the irradiation times to be comparable to the half lifetimes  $(T_{1/2})_i$  of various DN groups, as suggested by Keepin [1], one can choose to deal either with the contribution of the long-lived or with that of the short-lived groups to the DN emission. On the other hand, periodical irradiation of the target allows an equilibrium intensity of DN from all groups to be achieved in between the irradiation cycles. A method of periodical irradiation (MPI) was applied by Brunson and Huber [6] at their "bandsaw" facility and, later on, by Dowdy et al. [7].

Below a MPI of a fissionable isotope target by neutron bursts generated by the IBR-2 PR is briefly described.

The IBR-2 PR is used as a pulsed neutron source with a pulse frequency corresponding to the time interval  $T$  between the pulses. The exposure of a target is  $\Delta t$ , and the distance between the reactor core and the target is  $L$  metres. A SNC synchronized with the reactor bursts is used for terminating the reactor beam after a time of  $\Delta t$  and for absorption of the reactor DN. When the beam is cut off, measurement of the DN emission from the target in the time interval between  $t_1$  and  $t_2$  is initiated by means of an ND. A simplified layout of the IBR-2 core, the SNC and the ND is shown in Fig. 1. Since the IBR-2 is used as a pulsed neutron source and both the PR and the SNC are synchronized, the expected time distribution of detected neutrons should consist of two different parts. The first part includes prompt fission neutrons (FN) detected during the exposure time  $\Delta t$ . Since the FN are "time markers" of fission events caused by reactor neutrons, this part of time distribution can be considered as a time-of-flight (TOF) reactor neutron spectrum. The second part represents the time distribution of detected DN in the time interval  $t_1 - t_2$ , when the reactor neutron beam is cut off and this distribution has no connection with the TOF method. However, below we shall quite arbitrarily refer to such a time distribution of either detected FN or DN as the "TOF neutron spectrum". The simplified expected TOF neutron spectrum is shown in Fig. 2.

The peak of area  $S(\text{FN})$  corresponds to the irradiation of a target with reactor beam neutrons. The area  $S(\text{DN})$  is defined as the sum of DN detected in the time interval  $t_1 - t_2$ , where  $t_2 < T$ . The number of fission events  $N_f$  caused by reactor neutrons during the exposure time is given by the following equation:

$$N_f = \frac{S(\text{FN})}{\epsilon(\text{FN}) \cdot \nu} \quad (1)$$

Since the ND detects DN periodically only within the time interval  $t_1 - t_2$  with  $t_2 < T$ , instead of a time interval  $t_1 - t_2$  with  $t_2 \rightarrow \infty$ , one must introduce a correction factor  $F(T, \Delta t, t_1, t_2)$  for determination of DN:

$$N_{\text{DN}} = \frac{S(\text{DN})}{\epsilon(\text{DN})} \cdot F(T, \Delta t, t_1, t_2), \quad (2)$$

Here

$$S(\text{DN}) = \int_{t_1}^{t_2} f_{\text{DN}}(t) \cdot dt,$$

where  $f_{\text{DN}}(t)$  is a time distribution function of DN.

In both equations (1) and (2) the quantities  $\epsilon(\text{FN})$  and  $\epsilon(\text{DN})$  are the efficiencies of the ND for FN and DN, respectively. Then the effective fraction of DN,  $\beta_{\text{eff}}$ , results from equations (1) and (2):

$$\beta_{\text{eff}} = \frac{S(\text{DN})}{S(\text{FN})} \cdot \frac{\epsilon(\text{FN})}{\epsilon(\text{DN})} \cdot F(T, \Delta t, t_1, t_2). \quad (3)$$

For the value of  $F(T, \Delta t, t_1, t_2)$  one can readily obtain the following expression, which takes into account periodical exposure of the target and the existence of 6 groups of DN, as suggested by Keepin [1]:

$$F(T, \Delta t, t_1, t_2) = \left[ \sum_{i=1}^6 \frac{A_i}{\lambda_i} \cdot \frac{1 - e^{-\lambda_i \Delta t}}{1 - e^{-\lambda_i T}} \cdot (e^{-\lambda_i t_1} - e^{-\lambda_i t_2}) \right]^{-1} \quad (4)$$

Here  $A_i$  is the relative yield and  $\lambda_i$  is the decay constant for the  $i$ -th group of DN. Setting the values of  $T = 200$  ms,  $\Delta t = 20$  ms,  $t_1 = 50$  ms and  $t_2 = 200$  ms, which is typical for the IBR-2 PR and the SNC, one can find the terms  $F'_i$ , where

$$F'_i = \frac{1}{\lambda_i} \cdot \frac{1 - e^{-\lambda_i \Delta t}}{1 - e^{-\lambda_i T}} \cdot (e^{-\lambda_i t_1} - e^{-\lambda_i t_2}), \quad (5)$$

to vary within several percent from the 1-st to the 6-th group of DN. This means that the contribution of each DN group to the total yield corresponds to its relative yield  $A_i$ . It is to be noted that this is an important preference of the MPI for determination of the  $\nu_{\text{DN}}$  values. Since the contribution of the 6-th group with the shortest half-lifetime becomes

significant, one can make a consistency check of the measured  $\nu_{DN}$  value with the recommended  $\lambda_g$  and  $A_g$  values [1, 2].

### III. Experimental set-up

Below one can find some physical characteristics of the PR and a brief description of both the SNC and the ND, which are the main parts of our experimental facility at the reactor neutron beam  $N^0 = 11$ .

The PR IBR-2 [8]. It exhibits an average thermal power of 2 MW, a peak power of 1500 MW, and the power released between pulses is  $\approx 0.1$  MW. This provides a thermal neutron flux density from the surface of the reactor moderator at the burst maximum of about  $10^{16}$  n/cm<sup>2</sup>·s. The repetition rate of neutron pulses is 5 Hz and the half-width of the fast neutron pulse is 215  $\mu$ s.

The SNC. A simplified cross section of the SNC, the collimators, the neutron guide pipes and the ND is depicted in Fig. 3. The SNC consists of a horizontal-axis cylindrical rotor made of borated polyethylene and steel, a stepping electric motor and electronics, which synchronizes rotation of the SNC rotor with the reactor neutron bursts. The distance between the reactor core and the middle of the SNC rotor is 7 metres long. To achieve a reasonable compromise between the exposure  $\Delta t$  of the target and the counting rate of the ND, the distance  $L$  between the reactor core and the target is chosen to be  $L = 16$  metres. Since the TOF spectra are expected to be smooth, a value of  $\Delta t/L \approx 1$  ms/m seems to be sufficient, even for the 6-th group of DN with  $T_{1/2}^{(6)} = 230$  ms [2].

Collimation of the reactor neutron beam behind the SNC is provided by a collimator system mounted between the SNC and the neutron guide pipe. Both the SNC rotor hole and the holes in the collimators are of a trapeze shape and have the same size. More details regarding the construction of collimators and their dimensions are presented in Fig. 4.

The electronics synchronization system allows the phase (expressed in time units) between the reactor burst and the position of the rotor hole to vary from 10  $\mu$ s up to 100 ms. By slowing down the rotation frequency (RF) of the SNC rotor from 5.0 Hz to 2.5 Hz; 1.66 Hz; 1.25 Hz; 1.0 Hz one may increase the time interval  $T$  between the neutron bursts from

200 ms up to 1 s. However, the exposure time  $\Delta t$  of the target is, then, enhanced proportionally.

ND. The ND is of the same type as previously described by Macklin et al. [9], Dowdy et al. [7] and by Avdeev et al. [10]. It is a multicounter detection system, which consists of 36 <sup>3</sup>He filled proportional counters, a 45 x 45 x 50 cm polyethylene moderator with 36 holes, for inserting the <sup>3</sup>He counters, and detector electronics.

The moderator has a central hole of diameter 14 cm intended for introduction of various samples: fissioned isotope targets, scatterers etc. The central hole is surrounded by two concentric rings of "counter" holes 22.5 cm and 33.5 cm in diameter.

All the utilized <sup>3</sup>He filled proportional counters are of the SNM-33 type (Russian made), 3.2 cm in diameter, 52 cm long, with a gas pressure of 2 atm and an operating voltage equal to 1850 V.

At present we use a simplified version of our ND with only 12 proportional counters inserted into the holes that form the inner ring.

All the sides of the polyethylene moderator are shielded with a 0.5 mm thick Cd cover and 5 cm thick borated polyethylene plates, that provide an effective protection of the ND against scattered neutrons. To reduce the background due to thermal neutron scattering on the target the central hole is also covered with 0.5 mm thick Cd shielding.

A partly dismantled ND is shown in Fig. 5. The pipe containing a measured sample is withdrawn from the central hole. During measurements the pipe is evacuated down to a vacuum of about  $10^{-2}$  mm Hg, which reduces the neutron background at the ND. A BF<sub>3</sub> gas filled proportional counter used as a neutron flux monitor is mounted on the pipe's flange.

The 12 <sup>3</sup>He proportional counters are divided into 4 groups of 3 counters in each group. The detector electronics consists of 4 similar preamplifiers, amplifiers and discriminators, a logic "OR" unit and a HV supply. The number of counter groups chosen for reducing the drop in the neutron counting rate due to the pile up provides a reasonable compromise between the loss of experimental information and the cost of the electronics. All experimental information (ND counts, neutron beam monitor data) is collected by a computerized measurement module (CMM), which represents the measurement data in the form of TOF neutron spectra. All

"START" pulses triggering the CMM electronics are synchronized with the IBR-2 neutron bursts. However, when the SNC works with a chopper  $RF < 5$  Hz, the CMM is triggered by every second, third etc. "START" pulse. A block diagram of the detector electronics is depicted in Fig. 6.

The counting characteristics of each group of  $^3\text{He}$  filled proportional counters are adjusted to be similar by using a Pu-Be neutron source placed at the middle of the axis of the ND central hole. When 12 counters are in operation, the neutron detection efficiency is found to be approximately 10%.

Most of the test measurements are done with a metal sample of highly enriched uranium, containing 7 g of  $^{235}\text{U}$ , and a small lead sample of 22.33 g used for determination of the neutron background.

Besides the above, a 6 cm thick Pb scatterer placed across the neutron beam is used for reducing the thermal neutron intensity and, hence, the pile up of detector and CMM electronics. Another way of reducing the neutron flux intensity behind the SNC consists in increasing the SNC phase relative to the reactor neutron burst. Owing to the shape of the reactor neutron spectrum, an increase of the phase reduces the intensity of a thermal neutron flux. Both methods for variation of the neutron intensity are applied in the test measurements described below.

#### IV. The SNC and ND test measurements

The main goal of the measurements described below is to obtain information on the counting rates of both FN and DN, on the realistic duration of the exposure,  $\Delta t$ , on the neutron background of our ND etc.

The TOF neutron spectrum shown in Fig. 7 is obtained at a fixed position of the SNC rotor and with a small lead scatterer inserted into the ND. A train can be seen of two reactor bursts and 4 much smaller "satellite" bursts in between the main bursts. This TOF spectrum also allows some estimations to be made of the reactor fast neutron background between the bursts, because the Cd shielding which covers the surface of the central hole inside the ND absorbs all the scattered thermal neutrons and hence strongly suppresses the thermal neutron background at the detector.

The complicated shape of the IBR-2 neutron TOF spectrum is an unpleasant disadvantage of this pulsed neutron source based on the IBR-2. It can, however, be discarded by combining the IBR-2 with the SNC, which is synchronized with the "main" IBR-2 neutron bursts.

The TOF spectra shown in Fig. 8 and Fig. 9 are measured with the  $^{235}\text{U}$  sample and the SNC in operation. Both measurements are performed with the same 5 Hz RF and two different rotor phases equal to 6 ms and to 10 ms, respectively. To reduce piling up the detector and the CMM electronics an additional 6 cm thick Pb scatterer is placed across the neutron beam, providing an attenuation of the neutron intensity by a factor of  $\approx 5$ . Comparison of both TOF spectra reveals that the larger rotor phase results in a further twofold reduction of the neutron flux. Even in this TOF spectrum a small pile up of the electronics can be found during the exposure. To avoid a pile up, an additional transmission measurement with a sufficiently thick lead scatterer in the beam, providing no pile up, is performed with the  $^{235}\text{U}$  sample in a ND. By using a low efficiency neutron flux monitor one can measure the counts of  $S(\text{FN})_{\text{Pb}}$  and the sum of monitor counts,  $(\Sigma N)_{\text{Pb}}$ . The real value of  $S(\text{FN})$  with no lead scatterer in the beam can be found from the following simple expression:

$$S(\text{FN}) = (\Sigma N) \cdot \left( \frac{S(\text{FN})}{\Sigma N} \right)_{\text{Pb}} \quad (6)$$

One can also conclude that variation of the rotor phase does not alter the neutron background and that the ratio  $R = (\text{DN} + \text{background}) / (\text{background})$  varies from  $\approx 4$  for a 30 - 63 ms time interval up to 10 for a 90 - 120 ms time interval.

Two other measurements were carried out under experimental conditions similar to the previous ones, but with the RF equal to 2.5 Hz and rotor phases equal to 10 ms and 15 ms, respectively. These two TOF spectra are shown in Figs. 10 and 11. Since the RF is half the previous value, the exposure is two times longer, although it still remains under 20 ms. The values of R are almost the same as for the previous TOF spectra.

The neutron background in the test measurements described above is determined by replacing the uranium sample with a small lead scatterer inserted in the ND. However, this does not permit avoiding an uncertainty that occurs, if the position of the scatterer is slightly shifted with respect to the location of the uranium sample inside the ND. Besides this, for correct measurements of  $\nu_{DN}$ (th) values one must take into account that part of fissions that is caused by all epithermal neutrons, in spite of the number of such events expected to be very small.

The most convenient way of determining the neutron background would be to perform a "background" measurement with a Cd filter in the neutron beam. Test measurements with and without a 2 mm thick Cd filter in the beam are briefly described below. The TOF spectra with 2.5 Hz and 5.0 Hz SNC RF are shown in Figs. 12 and 13, respectively. The "background" curves from both spectra exhibit quite complicated shapes. Therefore, subtraction of the background requires accurate normalization of the "background" curve to the "DN + background" curve. To avoid possible variations of the IBR-2 reactor power during prolonged measurements the neutron flux monitor counting rates  $(\Sigma N)$  and  $(\Sigma N)_{Cd}$  obtained in "without Cd" and "with Cd" measurements can be utilized. Another way of normalization consists in comparison of the satellite peak areas from both the "DN + background" and "background" curves, which are used as "natural" flux monitors. The "pure" DN spectra shown in Fig. 14 represent a result of a "satellite" normalization and subtraction of the corresponding neutron backgrounds. The curve (1) in Fig. 14 is distorted by a pile-up of detector and CMM electronics caused by the approximately 16-fold higher counting rate as compared with the "2.5 Hz" measurement, i.e. the curve (2). Such a counting rate is a result of the following measuring conditions: a) doubled SNC rotor RF; b) the 6 cm thick Pb scatterer is withdrawn from the reactor neutron beam; a minimum rotor phase delay of 3 ms is used.

Unlike curve (1), curve (2) looks smooth, as is to be expected of the sum of 6 decay curves with differing  $\lambda_i$  values [1,2]. However, the "quality" of curve (2) can be checked by using the following approximate test. Since curve (2) is measured during the very limited time interval  $t_1 - t_2 \cong 350$  ms, it can be roughly fitted with a line exhibiting a small negative slope.

The slope P can be calculated from the following equation:

$$P = \left[ \left( \frac{dN_{DN}}{dt} \right)_{t_1} - \left( \frac{dN_{DN}}{dt} \right)_{t_2} \right] / \left( \frac{dN_{DN}}{dt} \right)_{t_2} . \quad (7)$$

The counting rate  $(dN_{DN}/dt)_t$  of DN at a time t after the exposure  $\Delta t$  is

$$\left( \frac{dN_{DN}}{dt} \right)_t = N_f \cdot \sum_{i=1}^6 Y_i \cdot \frac{1 - e^{-\lambda_i \cdot \Delta t}}{1 - e^{-\lambda_i \cdot T}} \cdot (e^{-\lambda_i \cdot t_1}) . \quad (8)$$

Here  $N_f$  is the number of fission events during the exposure of the target and  $Y_i$  is the absolute yield of DN for the i-th group. Assuming  $\Delta t = 20$  ms and  $t_1 - t_2 = 350$  ms one can find that the value of P amounts to about 14%. This value is close to the slope that can be found from Fig. 14, which is  $\approx 12\%$ .

It is to be noted that as a result of test measurements it is clear that our facility has a good reserve of neutron flux intensity of a factor of  $\approx 10$ . An additional enhancement of the neutron counting rate by a factor of  $\approx 2$  can be achieved by expanding the exposure  $\Delta t$ , i.e. by increasing the width of the SNC rotor hole. Moreover, the values of  $\epsilon(DN)$  and  $\epsilon(FN)$  can be raised from 10% up to at least 30% by adding the remaining 24  $^3\text{He}$ -filled proportional counters.

It is also clear, that the fast neutron background can be strongly suppressed by improving the collimators between the reactor core and the SNC. In addition, it can be reduced by a factor of  $\approx 3-5$  by using a cooled  $\text{SiO}_2$  crystal as thermal neutron filters [11].

It is interesting to consider some other applications of our facility, which could arise, if the above mentioned improvements would be performed.

## V. Other applications

Here we shall briefly consider some other applications of the above described facility that may be useful for the following purposes.

### 1. Searching for other DN groups with half-lifetimes $T_{1/2} < 200$ ms.

Above it was shown that the exposure  $\Delta t$  of the target does not exceed

20 ms, in the case of  $RF = 5$  Hz, and the moment of termination of a neutron beam is well defined. Therefore, detection of DN emission can start several milliseconds after the exposure is terminated. This allows performance of a consistency check of both the measured  $\nu_{DN}$  value and the experimental decay curve by taking advantage of the 6-group approach and recommended  $\lambda_i$  and  $A_i$  [1, 2]. For this purpose decomposition of the experimental decay curve must be carried out applying known least-square fitting procedures. The unique possibility, provided by our facility, of extending the fitting of our experimental decay curve down to 20 - 30 ms, also allows checking the existence of a short-lived group (or even groups) of DN with  $T_{1/2} < 200$  ms. To make such a check more reliable, an improvement of the collimators between the reactor core and the SNC is in progress.

2. Measurements of  $\nu_{DN}(th)$  values for  $^{241}Am$  and  $^{237}Np$ . Further improvements of our facility would make possible new more accurate measurements of  $\nu_{DN}(th)$  values for  $^{241}Am$  and  $^{237}Np$ , which are subthreshold fissioning nuclei with very small thermal fission cross sections of 20 millibarn for  $^{237}Np$  [12] and  $\approx 3.1$  barn for  $^{241}Am$  [12]. Both elements form odd-odd compound nuclei,  $^{238}Np$  and  $^{242}Am$ , respectively, and the knowledge of  $\nu_{DN}(th)$  may be of some interest, also, for  $\nu_{DN}(A, Z)$  systematics [2].

Estimations show that a 100 h long measurement would allow collection of a total number of DN counts,  $S(DN)$ , of  $\sim 10^5$  from a 100 mg  $^{241}Am$  target and of  $\sim 6 \cdot 10^4$  DN from 7 g of  $^{237}Np$ .

3. Investigation of the  $^{241}Am$  fission isomer. An interesting extension of  $^{241}Am$   $\nu_{DN}(th)$  measurements would be a more complicated measurement for determination of the average number of prompt fission neutrons  $\nu_{i,j}$  per isomeric fission of the compound  $^{242}Am$  nucleus. Such an investigation would allow comparison of  $\nu$  and  $\nu_{i,j}$  values and the height  $E_{i,j}$  of the isomeric level of Strutinsky's double-humped fission barrier to be found [13]. For this purpose our facility seems to be the most convenient one, since the half-life of the  $^{242if}Am$  fission isomer is  $\sim 14$  ms [14]. More details concerning measurements of the  $\nu_{i,j}$  value for the  $^{241}Am(n,f)$  isomeric fission can be found in Ref. [13].

4. Searching for delayed gamma-ray emission in the  $\sim 10 - 10^3$  ms time interval. It is to be noted that most pulsed neutron sources or research reactors equipped with neutron beam choppers cannot provide  $\sim 1 - 5$  Hz repetition rates of neutron pulses and target exposures of  $\sim 10 - 20$  ms without large losses of neutron intensity resulting in its decrease by factors of  $\sim 10 - 100$ . Therefore, the IBR-2 PR combined with a SNC is, also, undoubtedly the most convenient pulsed neutron source for searching for delayed gamma-ray emission in the time interval of  $10 - 10^3$  ms.

An extension of the time between target exposures from 200 ms up to 1 s resulting from a change in the RF of our SNC from 5 Hz down to 1 Hz provides a unique possibility for studying  $(n, \gamma)$  and  $(n, f)$  reactions and, in particular, expected isomeric states with half-lives  $\sim 10 - 10^4$  ms.

According to Strutinsky's theory of a double-humped fission barrier, a fissioning nucleus reaching the isomeric level close to the bottom of the second well may either penetrate the outer barrier and fission or go back through the inner barrier and emit a gamma-ray cascade with a reduced total energy  $E_\gamma \cong E_{i,j}$ . Since the  $^{238if}Np$  fission isomer has not been yet observed and since  $^{242if}Am$  has the longest known half-life equal to 14 ms, one would expect delayed gamma-ray emission to exist and to be observable in the "ms - s" time interval. A search for a delayed gamma-ray cascade could be realized, also, by means of the "IBR-2 + SNC" facility.

5. Neutron activation analysis of  $^{235}U$ -containing samples. A non-destructive assay of  $^{235}U$ -containing samples would be an important application of the "IBR-2 + SNC + ND" facility. As in the previous measurements, samples are introduced into the ND to be exposed to the reactor beam neutrons. However, in this case one has to account for the total number of fission neutrons,  $S(FN)$ , detected during the exposure of the sample. The estimated sensitivity of our facility to the  $^{235}U$ -content amounts to a few milligrams per sample. Further improvement of the sensitivity requires that the fast neutron background be reduced. It is expected that the neutron background could be suppressed by a factor of  $\sim 3 - 5$  by using a cooled  $SiO_2$  crystal as a thermal neutron filter [11]. Then, the sensitivity could reach a value of  $\sim 0.1$  mg of  $^{235}U$  per sample.

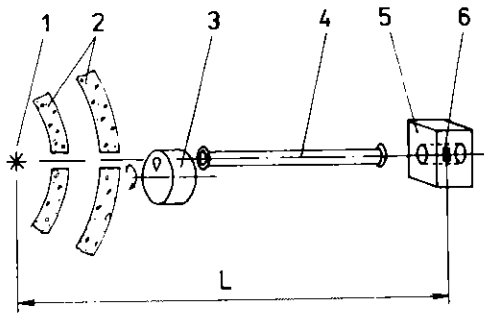


Figure 1. Schematic lay-out of the slow neutron chopper (SNC) and the neutron detector (ND) at the neutron beam of IBR-2 pulsed reactor (PR). 1 - reactor core; 2 - concrete shielding; 3 - SNC; 4 - neutron guide-pipe; 5 - ND; 6 - target; L - length of the neutron flight-path.

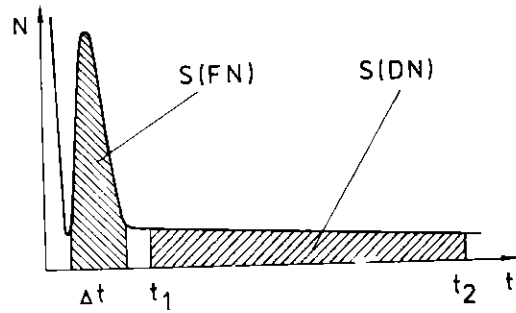


Figure 2. Time distribution of neutrons detected by ND after the IBR-2 START pulse.  $\Delta t$  - exposure time; S(FN) - peak area of fast neutrons detected during the exposure of a target; S(DN) - sum of delayed neutrons detected in a time interval  $t_1$ - $t_2$ , when the reactor neutron beam is cut off.

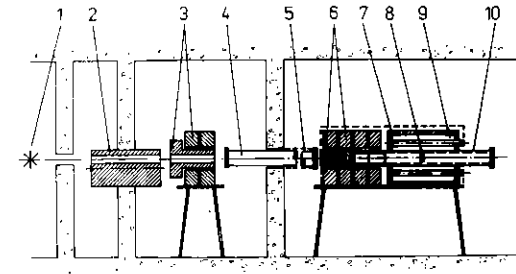


Figure 3. Sketch of the "SNC + ND" experimental arrangement : 1 - IBR-2 PR core; 2 - SNC; 3,6 - collimators; 4 - neutron guide-pipe; 5 - Cd shielding of guide-pipes, vacuum pipe and the ND; 7 - shielding of the ND; 8 - target; 9 - ND; 10 - vacuum pipe inserted into the ND.

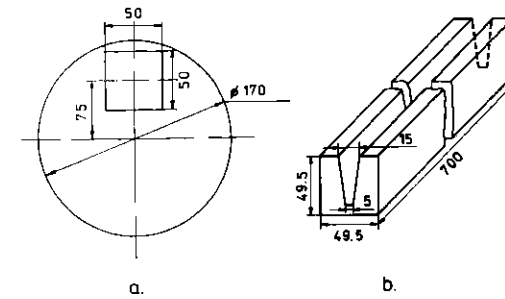


Figure 4. Sketch and dimensions of the SNC rotor (a) and rotor insertion (b).



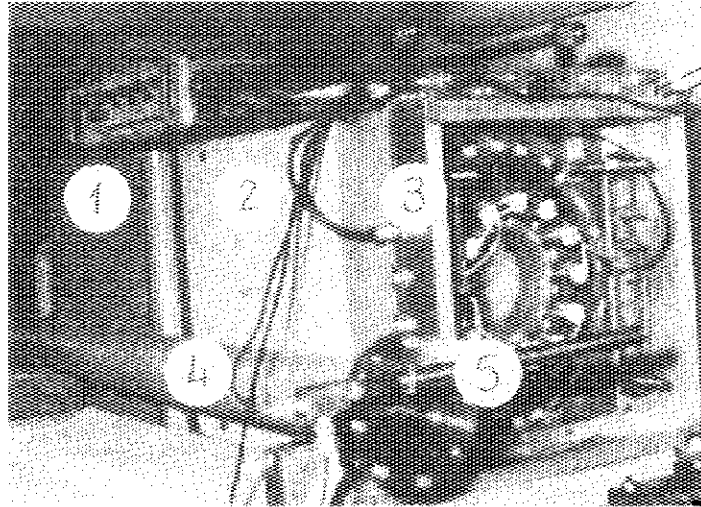


Figure 5. Partly dismantled ND with withdrawn vacuum pipe. 1 - collimators; 2 - shielding plates of the ND; 3 - the ND with  $^{12}\text{He}$  - filled proportional counters placed around the central hole; 4 - vacuum pipe; 5 - neutron flux monitor.

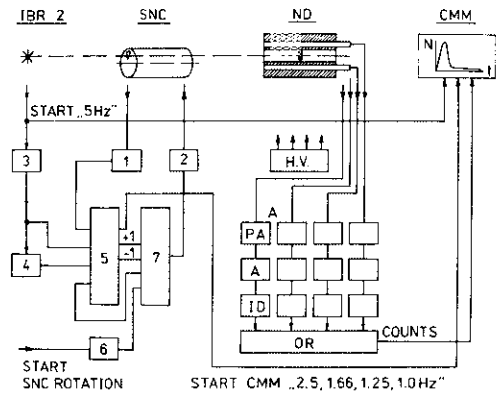


Figure 6. Block diagram of the SNC electronics and neutron detection system. 1 - the SNC frequency driver; 2 - stepping motor driver; 3 - rotor phase delay; 4,5 - synchronization system consisting of phase detector and comparator; 6 - SNC rotor accelerator driver; 7 - digital operation system of stepping motor; H.V. - high voltage supply; PA - preamplifiers; A - amplifiers; ID - integral discriminators; OR - logic OR.

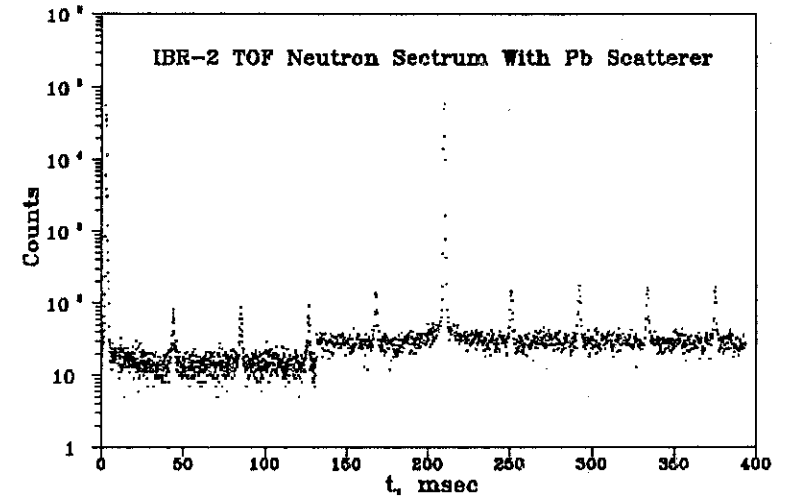


Figure 7: A TOF spectrum with fixed SNC rotor position. A lead scatterer in the ND detector. TOF channels:  $1024 \times 128 \text{mksec} + 1024 \times 256 \text{mksec}$ . Measurement time:  $T_m = 30 \text{min}$ .

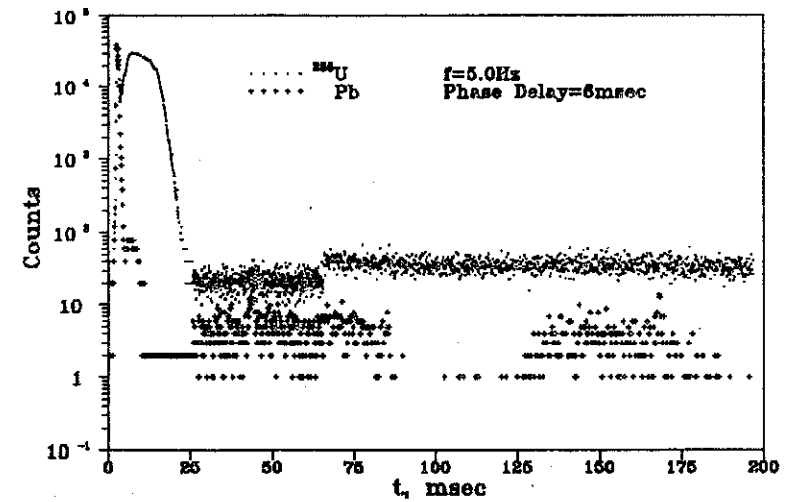


Figure 8: A TOF spectrum obtained at  $RF = 5 \text{Hz}$ ,  $T_m = 10 \text{min}$ , phase delay of 6 msec, 6cm thick Pb scatterer in the beam. TOF channels:  $1024 \times 64 \text{mksec} + 1024 \times 128 \text{mksec}$ .

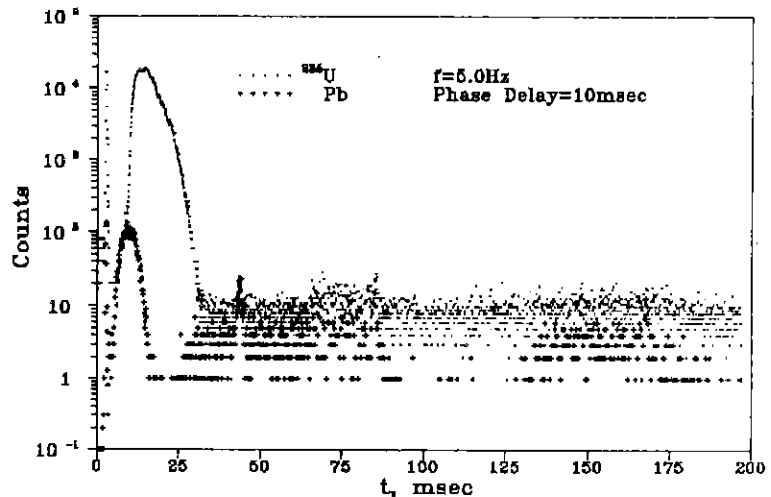


Figure 9: Measurement condition - as in Figure 8, except the phase delay of 10msec.

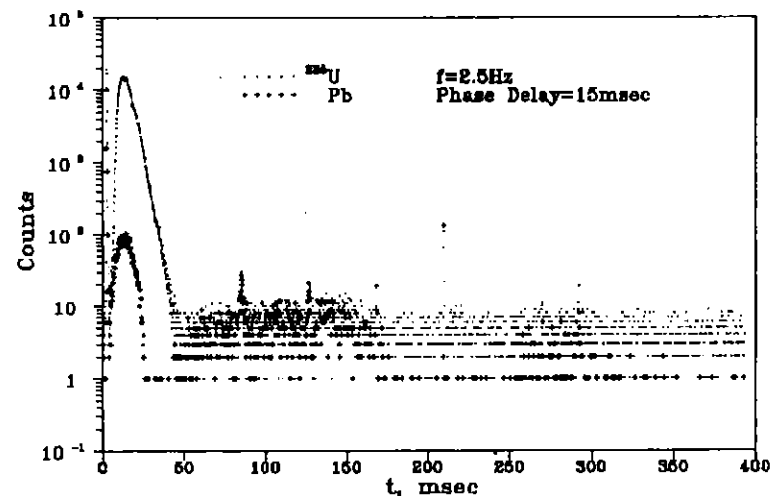


Figure 11: Measurement conditions as in Figure 10, except the phase delay of 15msec.

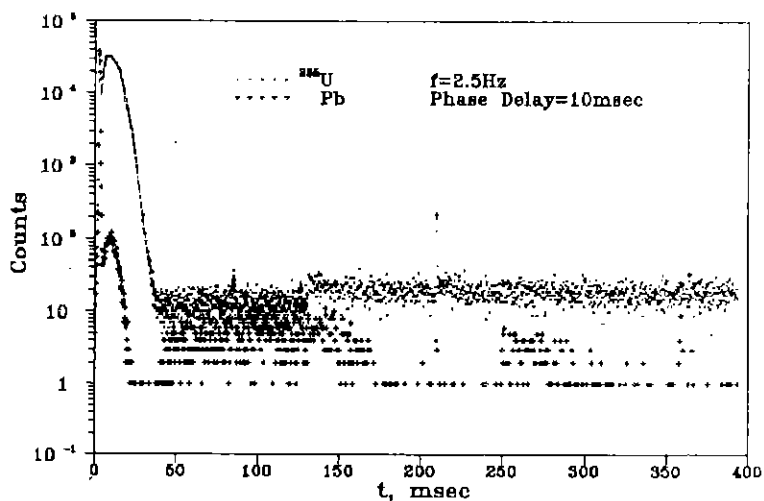


Figure 10: A TOF Spectrum obtained at RF=2.5Hz,  $T_m=10$ mm, phase delay of 10msec, 6cm thick Pb scatterer in the beam. TOF channels: 1024x128mksec + 1024x256mksec.

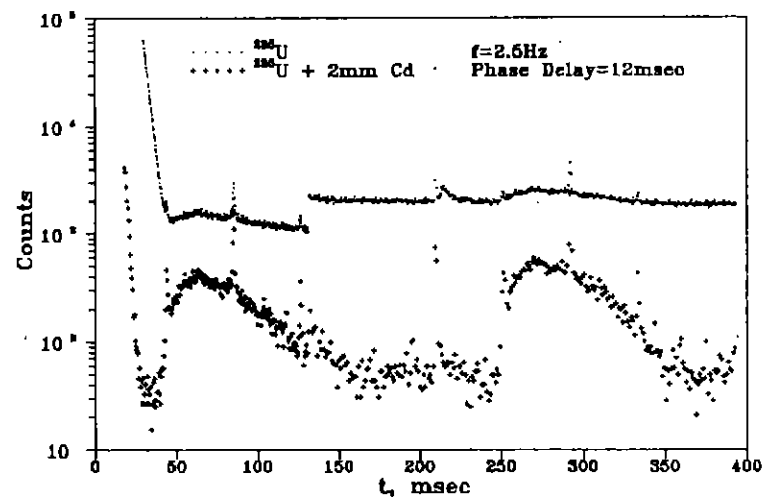


Figure 12: A TOF spectrum obtained at RF=2.5Hz,  $T_m=41$ h10min, phase delay of 12msec, 6cm thick Pb scatterer in the beam. Neutron background is measured with 2mm Cd filter,  $T_m=21$ h25min. TOF channels: 1024x128mksec + 1024x256mksec.

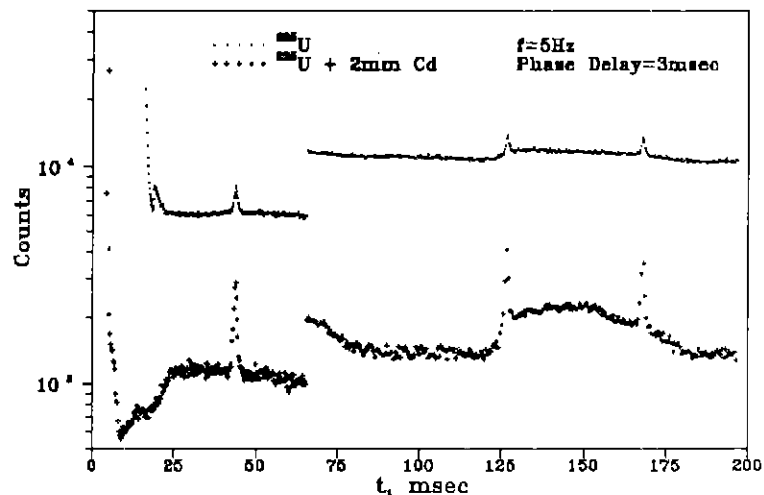


Figure 13: A TOF spectrum obtained at RF=5Hz,  $T_m=25h30min$ , phase delay of 3msec, the lead scatterer is withdrawn from the beam. Neutron background is measured with 2mm Cd filter,  $T_m=17h30min$ . TOF channels: 1024x64mksec + 1024x128mksec.

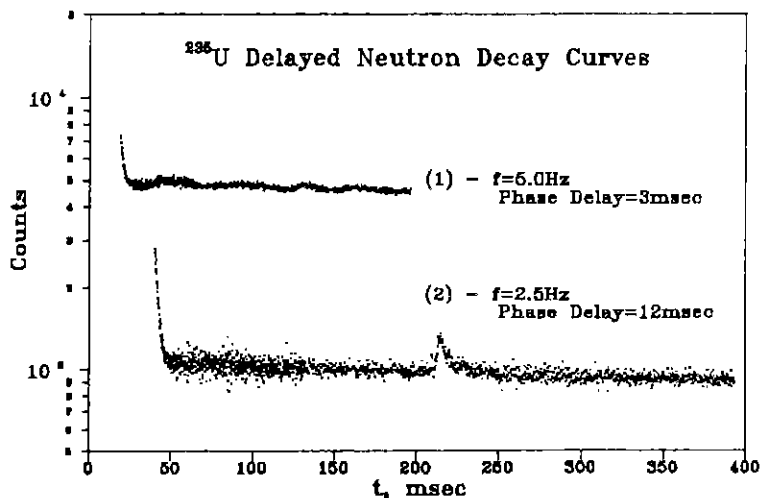


Figure 14: DN decay curves. Curves (1) and (2) are obtained at RF=5Hz and 2.5Hz, respectively.

## VI. Conclusions

A new facility for studying DN emission has been designed and tested, and a method for periodical irradiation of a target has been proposed and realized.

Comparing this facility with those used by other authors [2] one finds that it offers some unique experimental possibilities like the use of an extremely powerful pulsed neutron source based on the IBR-2 PR, the possibility of DN detection in between the neutron bursts starting a few ms after termination of the neutron beam by the SNC etc. Combination of the IBR-2 PR with the SNC allows the time interval between periodical exposures to be extended up to 1 s. In spite of these, and some other, advantages, we would like to note that the most effective would be to use this facility together with other methods for  $\nu_{DN}$  measurements, which would allow the duration of the exposure and the measuring time to be varied within wide limits: from some ms up to several minutes, and, therefore, different groups of DN to be studied.

We would also like to note that this is actually a multipurpose facility, which could be utilized in solving some other problems relevant to nuclear fission,  $(n, \gamma)$ -reactions etc.

## VII. Acknowledgments

The authors wish to express their gratitude to Dr. Alexandre Filip, Dr. L.B. Pikelner and Dr. W.I. Furman for their suggestions and continuous interest in this work. We are also indebted to Dr. Yu.V. Grigoryev for providing us with the uranium sample. The help of Mr. S.B. Borzakov in some of the test measurements is appreciated.

## VIII. References

1. G.R. Keepin, Physics of Nuclear Kinetics, Addison Wesley, Reading, mass. (1965).
2. R.J. Tuttle, Nucl.Sci.Eng., **56**, 37 (1975).

3. V.M. Sluचेvskaja, J.P Matveenko, Problems of Nucl.Sci. and Technique, Nucl.Data, v.3(38), 29 (1980), Moskow, USSR.
4. J. Blachot, M.C. Brady, A. Filip, R.W. Mills, D.R. Weaver, OECD-NEA, NEACRP-L-323,1990.
5. A. Filip, A. D'Angelo, "Nuclear data for Science and Technology", Proceedings, FRG, Juelich, 13-17 May 1991, p.946, Springer-Verlag, Berlin.
6. G.S. Brunson, R.J. Huber, "Delayed Fission Neutrons", Proc. of a Pannel, Nienna, 24-27 April 1967, p.229, IAEA, Vienna, 1968.
7. E.J. Dowdy, J.T.Caldwell, G.M. Worth, Nucl.Instr.Meth., **115**, 573 (1974).
8. User Guide. Lab. of Neutron Physics, JINR, 1991, Dubna, Russia.
9. R.L. Macklin, F.M. Glass, J. Halperin, R.T. Roseberry, H.W. Schmitt, R.W. Troughon, M. Tobias, Nucl.Instr.Meth., **102**, 181 (1972).
10. S.P. Avdeev, A.T. Vasilenko, V.A. Karnauchov, V.D. Kuznetsov, G.V. Mishinsky, L.A. Petrov, JINR, P13-86-456, Dubna, 1986.
11. A.K. Freund, Nucl.Instr.Meth., **213**, 495 (1983).
- 12 V.M. Gorbachov, Y.S. Zamyatnin, A.A. Lobov, "Nuclear Reactions in Heavy Elements" (A data Handbook), Pergamon Press, 1980.
13. E. Dermendjiev, Proc. of Vth Int.Symp. on the Interactions of Fast Neutrons with Nuclei, November 17-21, 1975, Gaussig, DDR, Report ZfK-324, p.169, Dresden, 1976.
14. S.M. Polikanov et al. Sov. JETP, **42**, 1964 (1962).

Received by Publishing Department  
on January 11, 1993.